Sub-10 nm Electron Beam Nanolithography Using Spin-Coatable TiO2 Resists

ARTICLE *in* NANO LETTERS · NOVEMBER 2003

Impact Factor: 13.59 · DOI: 10.1021/nl034584p

NANO LETTERS

2003
Vol. 3, No. 11
1587−1591

Sub-10 nm Electron Beam Nanolithography Using Spin-Coatable TiO_2 Resists

M. S. M. Saifullah,*,† K. R. V. Subramanian,† E. Tapley,‡ Dae-Joon Kang,† M. E. Welland,† and M. Butler‡

The Nanoscience Centre, Interdisciplinary Research Collaboration in Nanotechnology, University of Cambridge, 11 J. J. Thomson Avenue, Cambridge CB3 0FF, United Kingdom, and Leica Microsystems Lithography Limited, P.O. Box 87, Coldhams Lane, Cambridge CB1 3XE, United Kingdom

Received July 29, 2003; Revised Manuscript Received September 16, 2003

ABSTRACT

Conventional methods for electron beam patterning of TiO_2 are based on sputtering and lift-off. This poses significant problems in producing high aspect ratio and stoichiometric structures, especially in the sub-100 nm size range. We describe an alternative approach of preparing spin-coatable TiO_2 resists by chemically reacting titanium *n*-butoxide with benzoylacetone in methyl alcohol. They have an electron beam sensitivity of $\sim$35 mC cm^{-2} and are >10^7 times more sensitive to an electron beam than sputtered TiO_x and crystalline TiO_2 films. Fourier transform infrared studies suggest that exposure to an electron beam results in the gradual removal of organic material from the resist. This makes the exposed resist insoluble in organic solvents such as acetone, thereby providing high-resolution negative patterns as small as 8 nm wide. Such negative patterns can be written with a pitch as close as 30 nm.

1. Introduction. Titanium dioxide has shown its potential application in solar cells,[1,2] optical waveguides,[3−5] gas sensors,[6] and electrochromic displays.[7,8] One of the hindrances for miniaturization of these devices is the lack of an easy and reliable way of patterning TiO_2. Conventionally, TiO_2 is patterned by sputtering it on to a prepatterned organic resist and then performing lift-off. But the lift-off process remains delicate, especially when complicated features and/or thick films of TiO_2 are desired. To eliminate the problems associated with lift-off, we propose a sol−gel-based spin-coatable TiO_2 resist that is not only amenable to direct-write using an electron beam but is also capable of providing sub-10 nm resolution.

Very few studies have been carried out on electron beam patterning of sol−gel derived metal oxide resists, and nearly all of them are confined to spin-coatable Al_2O_3[9−13] and hybrid oxide resists.[14−16] Attempts have been made in the past to perform electron beam nanolithography on condensed titanium isopropoxide films to obtained TiO_2 patterns.[17−19] These films showed a high sensitivity to an electron beam, but cumbersome deposition of titanium isopropoxide required a high vacuum chamber and cooling of the wafer for alkoxide deposition.

In this paper we describe a simple process of electron beam nanopatterning of a highly sensitive spin-coatable TiO_2 resist prepared by chemical modification of titanium *n*-butoxide, $Ti(OBu^n)_4$, with benzoylacetone, BzAc. The resist was found to be stable in air. Exposure to an electron beam results in the rapid breakdown of organic bonds in TiO_2 resist. Development of exposed resist resulted in negative patterns with line widths as small as 8 nm.

2. Experimental Procedure. The three important criteria for obtaining a good spin-coatable resist are its stability in solution, stability in laboratory atmosphere after coating, and its development characteristics. To optimize the stability of the resist in a solution, a series of experiments were carried out. Equimolar amounts of $Ti(OBu^n)_4$ and various β-ketoesters (methyl acetoacetate, ethyl acetoacetate, isopropyl acetoacetate, isobutyl acetoacetate, and isoamyl acetoacetate) and β-diketones (acetylacetone, AcAc, and BzAc) were reacted in methyl alcohol (MeOH) for 2 h at room-temperature inside a glovebox (<5% relative humidity). It was observed that stabilizing $Ti(OBu^n)_4$ with β-ketoesters resulted in the precipitation in the solution and these solutions were discarded. On the other hand, the β-diketone stabilized $Ti(OBu^n)_4$ gave clear solutions. However, AcAc-stabilized $Ti(OBu^n)_4$ gave poor development characteristics as opposed to BzAc-stabilized $Ti(OBu^n)_4$. Hence only the latter was chosen for further studies.

* Corresponding author. E-mail: msms2@eng.cam.ac.uk
† University of Cambridge.
‡ Leica Microsystems Lithography Limited.

10.1021/nl034584p CCC: $25.00
Published on Web 10/01/2003

For spin-coating on precleaned silicon wafers, the BzAc-stabilized $Ti(OBu^n)_4$ solution were diluted in 1-pentanol to achieve appropriate resist thickness. One set of coated wafers was baked at 80 °C for an hour. A modified JEOL 4000EX nanowriter operating at 100 kV was used to study the exposure characteristics of the resists. High-resolution nanolithography was carried out in a Leica VB6-UHR-EWF operating at 100 kV with a probe current of 1.5 nA. The exposed resists were developed in acetone and rinsed in 2-propanol (IPA) for 10 s each.

AFM studies were performed using a Digital Instruments nanoscope to determine the change in solubility after development of the electron beam exposed TiO_2 resists. A LEO scanning electron microscope (SEM) was used to study the developed patterns.

A Mattson Instruments 4020 Galaxy series Fourier transform infrared (FTIR) spectrophotometer was used to carry out studies to determine the environmental stability as well as electron beam damage characteristics of spin-coatable TiO_2 resists.

3. Results and Discussion. Metal alkoxides such as $Ti(OBu^n)_4$ are very reactive compounds because of the presence of electronegative alkoxy groups, making the metal atoms highly prone to nucleophilic attack. Due to the high affinity of $Ti(OBu^n)_4$ to water, the hydrolysis reaction results in the formation of molecular aggregates of hydrated titanium oxide alkoxides. However, under carefully controlled conditions it is possible to form soluble polymeric intermediates (or sol) which undergo further polymerization to form a clear gel. In the present study, the hydrolytic reactivity of $Ti(OBu^n)_4$ was controlled by complexation with BzAc, a β-diketone capable of keto−enol tautomerism, as shown in eq 1.

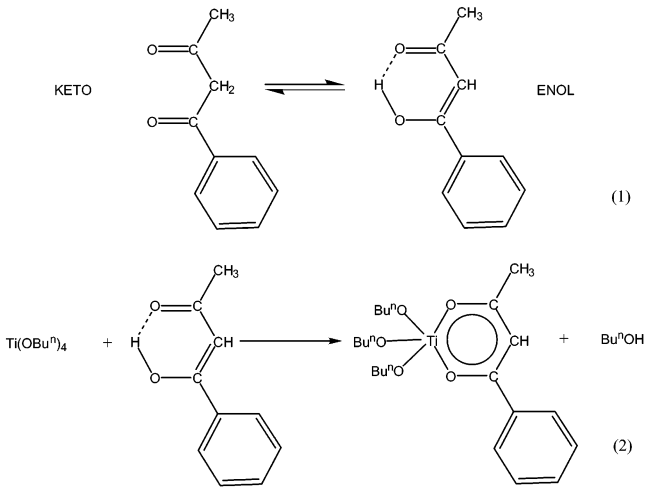

The enol form of BzAc is stabilized by chelation with $Ti(OBu^n)_4$. Further, the reaction also results in the partial replacement of the alkoxyl group by a β-diketonato ligand, as shown in eq 2. The hydrolytic activity of stabilized $Ti(OBu^n)_4$ is substantially reduced−perhaps due to the steric hindrance. However, it does not prevent the approach of water molecules that gradually replace the alkoxide groups with OH groups or which attack the chelate rings.

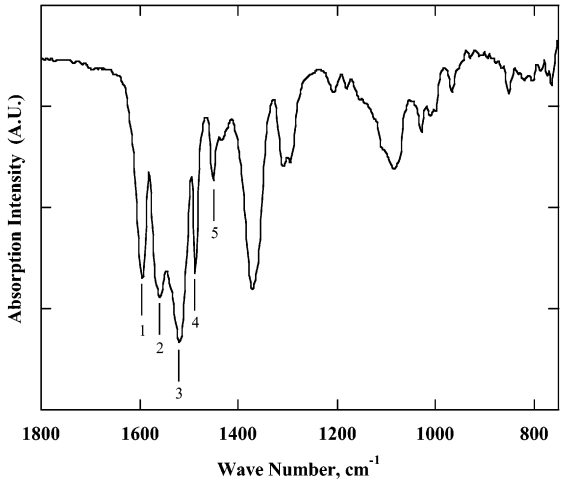

Figure 1. Characteristic infrared absorption peaks of spin-coatable TiO_2 film. The principal peaks are identified in Table 1.

Table 1: Characteristic Infrared Absorption Peaks of Spin-Coatable TiO_2 Film[a]

absorption peak, cm^{-1}	assignment	peak number
1595	ν(C== O)	1
1520	ν(C== C)	2
1559, 1484	Phenyl	3, 4
1448	C−H and C=O	5

[a] Only prinicipal peaks are identified.

Figure 1 shows the FTIR spectrum of a spin-coatable TiO_2 resist, and Table 1 provides identification of its principal absorption peaks. The IR spectrum shows a large number of absorption bands/peaks between 750 and 1800 cm^{-1}. The pair of absorption peaks observed at 1595 cm^{-1} and 1520 cm^{-1} is attributed to the bidentate character of metal-bonded BzAc and hence is indicative of the formation of the chelate complex. These peaks correspond to the ν(C== O) and ν(C== C) vibrations of the chelate ring, respectively.

The atmospheric stability of spin-coatable TiO_2 resist under laboratory conditions (25 °C, ∼30% relative humidity) is shown in Figure 2. The stability of the TiO_2 resist is dependent upon the stability of the chelate rings with respect to moisture in a laboratory atmosphere. It is seen that the peaks associated with chelate rings, viz., ν(C== O) and ν(C== C) hardly show any change in intensity even when exposed for 24 h, thereby proving their high stability.

Spin-coatable TiO_2 resists of ∼30−45 nm thickness were obtained by diluting the original solution in 1-pentanol and spin-coating it on a silicon wafer. The coated resist was exposed to an electron beam at different doses, developed in acetone, and rinsed in IPA. Negative type patterns were obtained after development. AFM studies were carried out to measure the height of these patterns formed due to difference in exposure doses. Figure 3 shows the exposure response curves of unbaked and baked spin-coatable TiO_2 resists. It is seen that the sensitivity and contrast of the resists is ∼35 mC cm^{-2} (at $D_{0.5}$) and contrast (γ) = 1, respectively. Baking at 80 °C for an hour does not seem to affect either sensitivity or contrast.

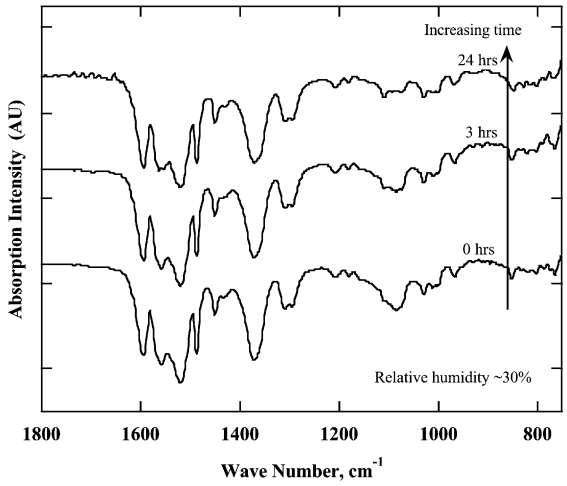

Figure 2. FTIR spectra showing the atmospheric stability of spin-coatable TiO_2 resist; as coated, after 3 h and after 24 h in an atmosphere of 30% relative humidity.

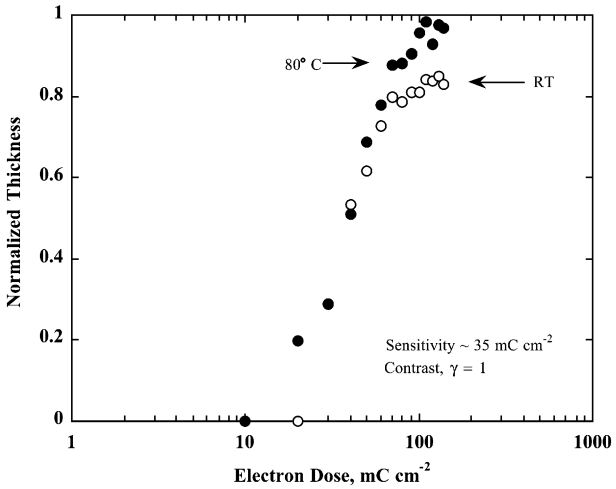

Figure 3. Exposure response curve of a spin-coatable TiO_2 resist showing the effect of baking temperature. The sensitivity is measured at half the height of normalized thickness.

The spin-coatable TiO_2 resists are $>10^7$ times more sensitive to an electron beam than are sputtered TiO_x and crystalline TiO_2 films.[20] Thus, spin-coatable TiO_2 resists provide not only the ease of deposition but also very high sensitivity when compared with sputter-deposited amorphous TiO_x and crystalline TiO_2 films.

The electron beam damage studies of spin-coatable TiO_2 resist were carried out by exposing a 200 μm × 200 μm area at 60 kV and conducting FTIR studies on it using an infrared microscope. Figure 4 shows the time-resolved FTIR spectra of spin-coatable TiO_2 resist acquired in reflectance mode. It was observed that, with increasing electron dose, the peaks in the range 1700 to 1100 cm^{-1} decrease in intensity. Among them are the peaks associated with the chelate ring as well as the phenyl group that undergo rapid breakdown under an electron beam. This damage mechanism is similar to that of spin-coatable Al_2O_3 resists.[10] The process of bond-breaking results in the formation of volatile compounds that are desorbed from the surface of the film in the high vacuum of the exposure machine. This results in the

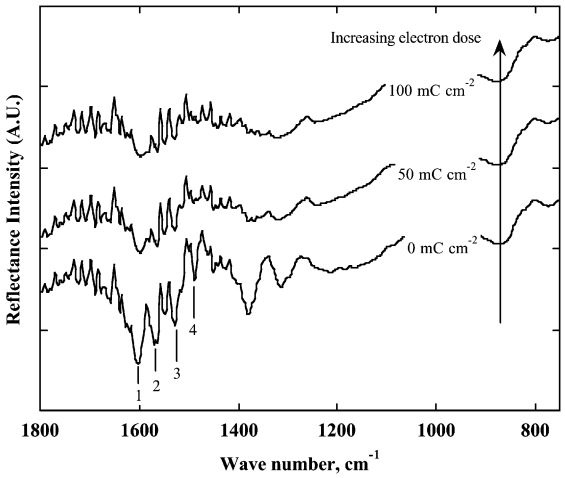

Figure 4. Time-resolved FTIR spectra of electron beam damage of spin-coatable TiO_2 resists. Table 1 lists the peak assignment.

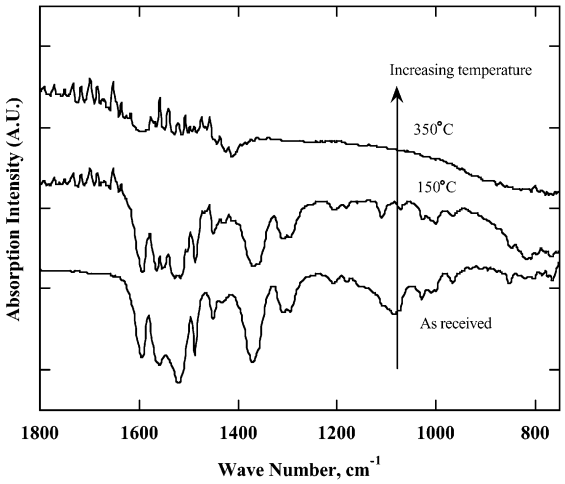

Figure 5. Effect of temperature on FTIR spectra of spin-coatable TiO_2 resists.

"flattening" of the FTIR spectra. Comparing Figure 3 and Figure 4, it can be seen that only a few chelate rings are required to be broken down in order to make the resist insoluble to organic solvents such as acetone. The disappearance of chelate rings is also observed when heating the spin-coatable TiO_2 resists (Figure 5). Heating the films above 500 °C in air results in pure titania films. However, the crystallization of nanostructures may occur at temperature much lower than 500 °C.

The electron beam damage behavior of spin-coatable TiO_2 resists is different from sputter-deposited TiO_2 films. The electron energy loss spectroscopy (EELS) studies on crystalline and amorphous TiO_2 films show that with an increasing electron dose, the crystal field split in Ti-$L_{3,2}$ edges disappears. Also, a shift of Ti-$L_{3,2}$ edges to lower energies (~2 eV) is seen, suggesting a reduction in the oxidation state of titanium.[20] The oxygen K-edge also shows a gradual disappearance of the crystal field split peak in both cases and reduces to a shoulder at a dose of 2×10^9 mC cm^{-2}. Such a shift in Ti-$L_{3,2}$ shows a transition from insulator to metal. A similar effect is observed in the irradiation damage of

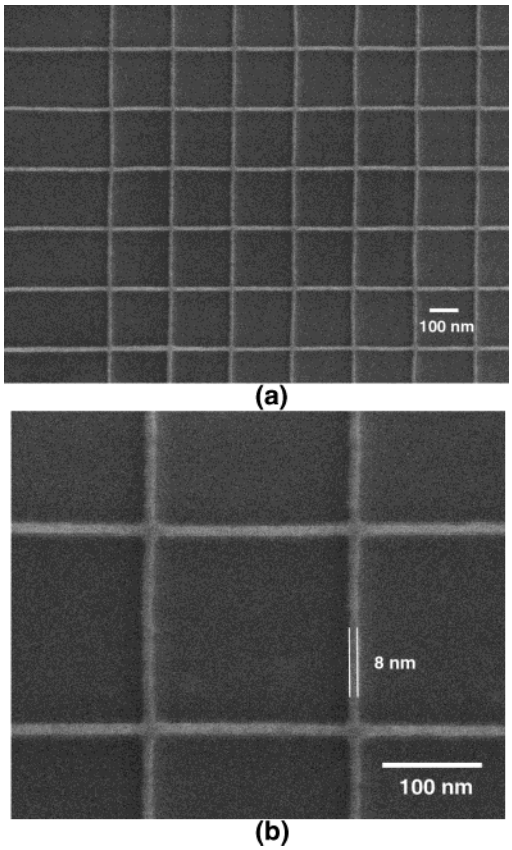

Figure 6. (a) SEM images of sub-10 nm patterned grid using a spin-coatable TiO_2 resist. (b) An 8 nm wide line.

amorphous SiO_2 where both the Si-$L_{3,2}$ and the Si-L_1 edges move to lower values as oxygen is lost from the irradiated area.[21]

High-resolution nanolithography was performed by writing continuous single pass lines across the entire 1200 μm field on pitches of 200 and 500 nm in a Leica VB6-UHR-EWF machine. The beam step size was 5 nm. Single pass lines require considerably more electron dose than writing large areas. A 10 $\times$ 4 array of fields were exposed with a start dose of 100 mC cm^{-2} and a dose increment of 1.05 per field. Each 1200 μm patterned field was stepped and settled within 200 ms. Figure 6a shows an SEM image of an array of sub-10 nm lines corresponding to an electron dose of 292.5 mC cm^{-2} ($\sim$ 146 nC cm^{-1}). The smallest line width obtained was 8 nm (Figure 6b) and the aspect ratio $\sim$4. The ability to write such fine lines is probably due to the combination of two factors: smaller molecular weight as well as smaller particulate size of BzAc-stabilized Ti(OBu^n)$_4$.

Pattern density studies were carried out by writing $\leq$ 10 nm wide lines with different pitches (Figure 7). It was found that the critical separation between the features was 30 nm. At 30 nm, a few cases of collapsing of the lines into each were seen (Figure 7c). This was perhaps due to a combination of various factors such as surface tension forces during development, blow drying, and insufficient dose. For the sake of comparison, in a negative PMMA resist, $\sim$12 nm features with 35 nm pitch were achieved after pattern transfer.[22]

Another important characteristic of spin-coatable TiO_2 resist is its ability to directly pattern large and complex

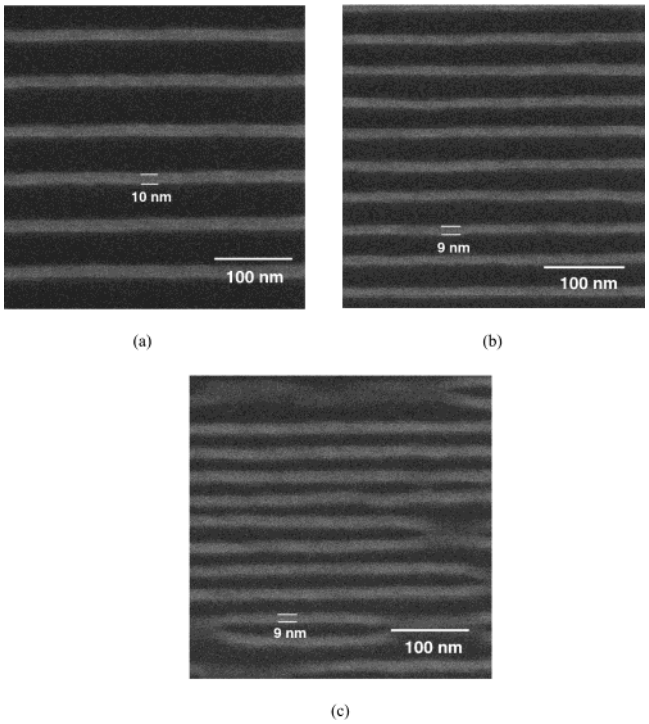

Figure 7. Patterning density of spin-coatable TiO_2 resist with (a) 60 nm, (b) 40 nm, and (c) 30 nm pitches. Conditions: dose = 292.5 mC cm^{-2}, beam step = 2 nm, and probe current = 2.18 nA.

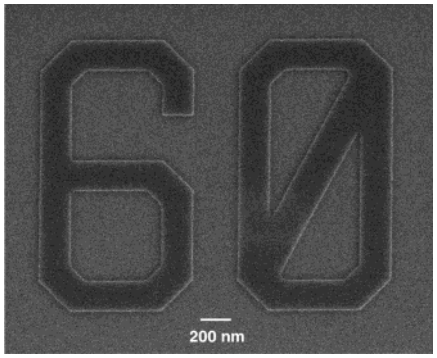

Figure 8. SEM image showing an example of close tolerances that can be achieved when directly writing complex features using a spin-coatable TiO_2 resist.

features with close tolerances at doses as low as 30 mC cm^{-2}. Figure 8 shows an SEM image of features written with a design width of 200 nm. It was observed that the deviation from the actual design width was well below 8%.

4. Conclusions. Spin-coatable TiO_2 resists obtained from chemical modification of Ti(OBu^n)$_4$ with BzAc were studied for the effects of electron beam on their chemical properties. The electron beam sensitivity of TiO_2 resist is $\sim$35 mC cm^{-2} and has a contrast (γ) = 1. These films are at least 10^7 times more sensitive to an electron beam when compared with amorphous TiO_x and crystalline TiO_2 films. Time-resolved electron beam damage studies suggest that the exposure of TiO_2 resist to an electron beam result in the disappearance of IR absorption peaks associated with the chelate ring. Exposure to the electron beam makes spin-coatable TiO_2 resists insoluble in acetone. This property was successfully employed to produce lines that were 8 nm wide. Features

that are ≤ 10 nm wide can be patterned with a 30 nm pitch. Large and complex features can be directly written with close tolerances. This technique offers a new and easy way of directly patterning complicated inorganic nanostructures for potential applications in solar cells and optical waveguides.

Acknowledgment. We thank Mohammad Khalafallah and Dr. David Hasko for their assistance in large area exposures and Laurent Costier for his assistance in FTIR studies.

References

(1) O'Regan, B.; Grätzel, M. *Nature* **1991**, *353*, 737.
(2) Barbé, C. J.; Arendse, F.; Comte, P.; Jirousek, M.; Lenzmann, F.; Shklover, V.; Grätzel, *M. J. Am. Ceram. Soc.* **1997**, *80*, 3157.
(3) Yoshida, M.; Prasad, P. N. *Chem. Mater.* **1996**, *8*, 235.
(4) Que, W.; Zhou, Y.; Lam, Y. L.; Kam, C. H. *Appl. Phy. A* **2001**, *73*, 171.
(5) Que, W.; Kam, C. H. *Opt. Eng.* **2002**, *41*, 1733.
(6) Arakawa, S.; Mogi, K.; Kikuta, K.; Yogo, T.; Hirano, S. *J. Am. Ceram. Soc.* **1999**, *82*, 225.
(7) Ohzuku, T.; Hirai, T. *Electrochim. Acta* **1982**, *27*, 1263.
(8) Livage, J. *Mater. Res. Soc. Symp. Proc.* **1986**, *73*, 717.
(9) Saifullah, M. S. M.; Namatsu, H.; Yamaguchi, T.; Yamazaki, K.; Kurihara, K. *Proc. SPIE* **1999**, *3678*, 633.
(10) Saifullah, M. S. M.; Namatsu, H.; Yamaguchi, T.; Yamazaki, K.; Kurihara, K. *Jpn. J. Appl. Phys.* **1999**, *38*, 7052.
(11) Saifullah, M. S. M.; Kurihara, K.; Humphreys, C. J. *J. Vac. Sci. Technol. B* **2000**, *18*, 2737.
(12) Yamazaki, K.; Saifullah, M. S. M.; Namatsu, H.; Kurihara, K. *Proc. SPIE* **2000**, *3997*, 458.
(13) Saifullah, M. S. M.; Kang, D.-J.; Subramanian, K. R. V.; Welland, M. E.; Yamazaki, K.; Kurihara, K. **2003**, accepted for publication in *J. Sol-Gel Sci. Technol.*
(14) Rantala, J. T.; Nordman, N.; Nordman, O.; Vähäkangas, J.; Honkanen, S.; Peyghambarian, N. *Electron. Lett.* **1998**, *34*, 455.
(15) Rantala, J. T.; Penner, R. S.; Honkanen, S.; Vähäkangas, J.; Fallahi, M.; Peyghambarian, N. *Thin Solid Films* **1999**, *345*, 185.
(16) Cheong, W. C.; Yuan, X.-C.; Koudriachov, V.; Yu, W. X. *Opt. Express* **2002**, *10*, 586.
(17) Mitchell, W. J.; Hu, E. L. *J. Vac. Sci. Technol. B* **1999**, *17*, 1622.
(18) Mitchell, W. J.; Hu, E. L. *Appl. Phys. Lett.* **1999**, *74*, 1916.
(19) Mitchell, W. J.; Hu, E. L. *J. Vac. Sci. Technol. B* **1999**, *20*, 596.
(20) Saifullah, M. S. M.; Boothroyd, C. B.; Botton, G. A.; Humphreys, C. J. *Inst. Phys. Conf. Ser* **1997**, *153*, 167.
(21) Saifullah, M. S. M.; Boothroyd, C. B.; Botton, G. A.; Humphreys, C. J. *Electron Microscopy 96*; Committee of European Societies of Microscopy, Brussels, **1998**, *2*, 123.
(22) Hoole, A. C. F.; Welland, M. E.; Broers, A. N. *Semicond. Sci. Technol.* **1997**, *12*, 1166.

NL034584P